Reactive Oxygen Species Production from

Secondary Organic Aerosols: The Importance of

Singlet Oxygen

- 4 Alessandro Manfrin¹, Sergey A. Nizkorodov², Kurtis T. Malecha², Gordon J. Getzinger¹,
 5 Kristopher McNeill¹, Nadine Borduas-Dedekind^{1,3}*
- 6 ¹ Institute for Biogeochemistry and Pollutant Dynamics, ETH Zurich, 8092 Zurich, Switzerland
- ² Department of Chemistry, University of California, Irvine, CA 92697, USA
- 8 Institute for Atmospheric and Climate Science, ETH Zurich, 8092 Zurich, Switzerland

10 ABSTRACT

1

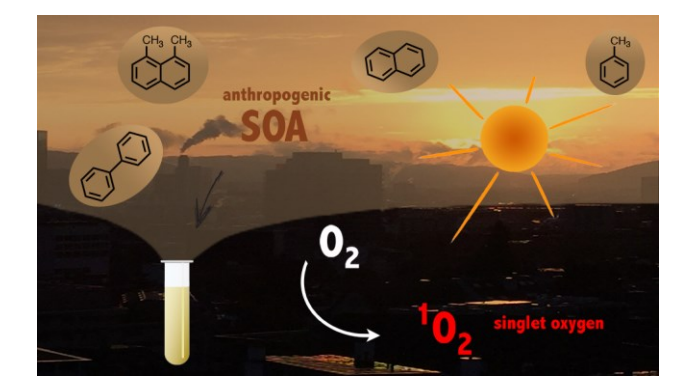
2

3

- Organic aerosols are subjected to atmospheric processes driven by sunlight, including the
- 12 production of reactive oxygen species (ROS) capable of transforming their physicochemical
- properties. In this study, secondary organic aerosols (SOA) generated from aromatic precursors
- were found to sensitize singlet oxygen (¹O₂), an arguably underappreciated atmospheric ROS.
- 15 Specifically, we quantified ${}^{1}O_{2}$, OH radical and $H_{2}O_{2}$ quantum yields within photoirradiated
- 16 solutions of laboratory-generated SOA from toluene, biphenyl, naphthalene, 1,8-
- 17 dimethylnaphthalene. At 5 mg_C L⁻¹ of SOA extracts, the average steady-state concentration of
- ¹O₂ and of OH radicals in irradiated solutions were $3 \pm 1 \times 10^{-14}$ M and $3.6 \pm 0.9 \times 10^{-17}$ M,
- 19 respectively. Furthermore, ROS quantum yields of irradiated ambient PM_{10} extracts were
- 20 comparable to those from laboratory-generated SOA, suggesting a similarity in ROS production
- 21 from both types of samples. Finally, by using our measured ROS concentrations, we predict that
- 22 certain organic compounds found in aerosols, such as amino acids, organo-nitrogen compounds

and phenolic compounds have shortened lifetimes by more than a factor of two when ${}^{1}O_{2}$ is considered as an additional sink. Overall, our findings highlight the importance of SOA as a source of ${}^{1}O_{2}$, and its potential as a competitive ROS species in photooxidation.

TOC art



INTRODUCTION

Organic aerosols are ubiquitous in the atmosphere and represent up to 90% of the submicron particulate mass. They can scatter solar radiation thereby impacting climate directly, but also act as cloud condensation nuclei and impact climate indirectly. It is thus important to understand the chemical and physical properties of organic aerosols and how these properties are modified by atmospheric processing, such as solar irradiation, heterogeneous oxidation, hydroscopic growth, aqueous phase processing, heterogeneous oxidation, also hydroscopic aerosols can proceed by gas phase partitioning and reactive uptake of oxidants such as hydroxyl radical and ozone. Yet, there is now a recognition that chemical reactions initiated within the particle phase can dominate aging processes and consequently alter the physicochemical properties of the aerosol. 10–12

The aqueous phase photochemistry of organic aerosols is driven by solar UV radiation and is thus limited to photons with wavelengths upwards of 290 nm. Direct photolysis of organic peroxides and of H₂O₂ can generate aqueous phase OH radicals, a highly reactive and unselective oxidant. Light absorption by chromophoric organic species can yield triplet state organic matter capable of oxidizing organic material as well as produce singlet oxygen ($^{1}O_{2}$). $^{13-15}$ Up to now, atmospheric $^{1}O_{2}$ has been quantified in cloud water, 16 fog water, 17,18 rain water 19 , in road dust 20 and very recently in particulate matter. 12 $^{1}O_{2}$ can also oxidize polyaromatic hydrocarbons within organic aerosols 21 to form secondary organic aerosol (SOA) from aqueous reactions of biogenic organic compounds. 22 Furthermore, $^{1}O_{2}$ is known to selectively undergo cycloaddition type reactions, which are well characterized in the context of biology. 23 This oxidant could be affecting the fate of aerosol tracers, of pollutants within aerosols and of toxins. 17,20,22 In addition, $^{1}O_{2}$ is an important oxidant when studying the fate of pollutants in aquatic environments such as surface waters as well as when understanding oxidative stress health complications within the human body. $^{10,1123-26}$

In aquatic environments, dissolved organic matter can sensitize ${}^{1}O_{2}$ with concentrations typically around 10^{-14} M. We hypothesized that ${}^{1}O_{2}$ could also be sensitized by chromophoric SOA. Indeed, we found that anthropogenic SOA produced from aromatic atmospheric precursors efficiently sensitized ${}^{1}O_{2}$ with quantum yields comparable to dissolved organic matter. Our goal was to quantify ${}^{1}O_{2}$ within irradiated SOA and particulate matter extracts, and to evaluate whether ${}^{1}O_{2}$ -mediated processes are competitive with other processes leading to the degradation of key organic aerosol tracers in SOA particles.

MATERIALS AND METHODS

1. SOA preparation and collection

The SOA samples were prepared by the photooxidation of toluene, biphenyl, naphthalene, 1,8-dimethylnaphthalene and α -pinene inside a smog chamber at UC Irvine using a previously described procedure. The aromatic compounds were chosen based on their hypothesized ability to form sensitizing molecules such as aromatic quinones as well as on their atmospheric relevance from anthropogenic sources. In addition, 1,8-dimethylnaphthalene was added to the list to investigate the role of 1,4-quinone type products on $^{1}O_{2}$ production. 1,8-Dimethylnaphthalene has two additional methyl groups preventing the formation of 1,4-quinone compared to naphthalene. Furthermore, α -pinene was chosen as a control non-aromatic precursor to generate SOA.

Briefly, aromatic compound vapors and oxidant precursor $H_{2}O_{2}$ were mixed in a 5 m 3 Teflon FEP. The chosen starting mixing ratios (Table S1) were relatively high to produce requisite

Briefly, aromatic compound vapors and oxidant precursor H₂O₂ were mixed in a 5 m³ Teflon FEP. The chosen starting mixing ratios (Table S1) were relatively high to produce requisite amount of material (~3 mg) for the photochemical experiments. The precursors was irradiated with UV-B lamps (centered at 310 nm; FS40T12/UVB, Solar Tec Systems, Inc.) for 2 to 3 hours at room temperature. Once sufficient particle mass concentration was achieved, the particles were collected on 0.2 μm pore size PTFE filters (FGLP04700 from Millipore) at 15 L/min for 3 to 4 hours (Table S1). The filters were vacuum sealed and kept frozen until extraction, and the extract solutions were stored at 4 °C (section 2 in SI).

2. Ambient PM sampling

PM₁₀ samples were collected on quartz microfiber filters 150 mm (Whatman[™]) with a High Volume Sampler Digitel DH 77 (Digitel Elektronik GmbH). 24-Hour PM₁₀ samples were taken on November 29th 2017 and on March 4th 2018, in Roveredo, in the canton of Graubünden in

Switzerland. Sampling dates were chosen when no extraordinary events occurred, and thus, the two selected filters can be regarded as typical particulate matter samples for this site (section 3 in SI fur further site details).

3. Extraction of SOA and PM₁₀ filters

Both the SOA and PM_{10} filters were extracted in glass Schott bottles with nanopure 18.2 ohm-cm milli-Q water and subsequently further diluted to exactly 5 mg_C L⁻¹. The submerged filters were then placed on a lab-shaker (Adolf Kühne AG) for about three hours at 250 rotations per minute to obtain the water extractable components. The filters were then removed using sterilized tweezers and the non-purgeable organic carbon (NPOC) content in the extracts was measured using a total organic carbon (TOC) analyzer (Shimadzu, model TOC-L CSH). NPOC calibrations were done with a recrystallized solution of dipotassium phthalate and NPOC detection limits of 1σ were < 0.01 mg C L⁻¹. Extracts were refrigerated at 4°C until use. We tested the effect of storage on the sensitizing ability of the solution, and concluded that no change in the sensitizing ability of the mixtures was observed after 1 month of storage (Table S3).

4. Irradiation experiments

All extracts and reference compounds were irradiated with a SMART narrow-band hand-held lamp at 311 nm at a distance of 2 cm from a rotating sample holder. Experiments measuring $^{1}O_{2}$ steady-state concentrations were also performed with ten bulbs of 365 nm UVA broad band in a Rayonet photoreactor for comparison. The relative intensity spectra of both the 311 nm lamp and the 365 nm broadband bulbs as a function of wavelength were recorded (Figure S4). For the determination of quantum yields, we favor the use of a single wavelength lamp over a broadband

source to simplify the rate of light absorption calculation, leading to fewer errors and thus more accurate quantum yield values. Furthermore, we argue that our quantum yield measurements represent upper limits due to the use of 311 nm wavelength, representing UVB irradiation, the highest energy range reaching the troposphere and the surface of the planet (Figure S2). Finally, the overlap between the SOA absorbance and the solar spectral flux is optimal between 310 nm and 340 nm (Figure S2), where the 311 nm lamp is indeed irradiating (section 4 in the SI).

120

121

122

123

124

125

126

127

128

129

130

131

132

133

134

135

136

114

115

116

117

118

119

5. Quantification of ¹O₂ steady-state concentrations

Steady-state ¹O₂ concentrations were determined for SOA extracts, solutions of SOA precursor compounds, solutions of two reference materials, specifically juglone and Suwannee River fulvic acid (SRFA), as well as extracts from two ambient PM₁₀ filters. Steady-state experiments were conducted at room temperature in individual borosilicate test tubes using furfuryl alcohol (FFA, 100 μM) as a probe for ${}^{1}O_{2}$, 28 and extracted organic material at a NPOC concentration of 5 mg_C L⁻¹ as the ¹O₂ sensitizer. The concentration of SOA samples was chosen (1) to be comparable to previously measured TOC for cloud waters, ²⁹ (2) to give measurable ¹O₂ production with consequent appreciable FFA degradation and (3) to operate at the exact same NPOC concentration for all extracts. Solutions were irradiated at 311 nm and 80 µL aliquots were sampled every 30 minutes and analyzed for FFA concentration using ultra high-pressure liquid chromatography (UPLC, Waters ACQUITY) coupled with a photodiode array detector (Figure S3). To account for the reaction of FFA with OH radicals, the FFA pseudo-first-order rate constants were corrected by subtracting the contribution of OH radicals to the observed decay of FFA according to $k_{obs}^{corr} = k_{obs}$ - $(k_{rxn}^{FFA,OH} \times [OH]_{ss})$, where $k_{rxn}^{FFA,OH} = 1.5 \times 10^{10} \text{ M}^{-1} \text{ s}^{-1}$, where

[OH]_{ss} is the concentration determined as described in section 7. Steady-state ${}^{1}O_{2}$ concentrations were calculated by dividing the corrected FFA pseudo-first-order rate constant $(k_{obs}{}^{corr})$ by its reaction rate constant with ${}^{1}O_{2}$ $(k_{rxn}{}^{FFA} = 1 \times 10^{8} M^{-1} s^{-1})$ as in equation (1).²⁸

140
$$[^{1}O_{2}]_{ss} = \frac{k_{obs}^{corr}}{k_{rxn}^{FFA}}$$
 (1)

By UPLC, the detection limit of FFA was 4×10^{-7} M, calculated using 3σ of the smallest FFA calibration peak divided by the calibration slope, which corresponds to a minimum detectable 1 O₂ steady-state concentration of 3×10^{-15} M. The kinetic solvent isotope effect was used to rule out FFA degradation by other oxidants, mainly triplet state organic. 30 According to Davis et al., 31 if FFA degradation is solely due to 1 O₂ oxidation, the FFA pseudo-first-order rate constant in a solvent mixture 1:1 D₂O/H₂O (v/v) should be 1.9 times the rate observed in pure H₂O, due to the difference in 1 O₂ lifetime in H₂O and D₂O. Therefore, we performed the FFA degradation experiments in 1:1 D₂O/H₂O (v/v) and found that FFA degradation is due solely to 1 O₂ for all SOA mixtures and PM₁₀ filters when irradiating at 365 nm, while there is a contribution of OH radical at 311 nm (Table S4).

6. Determination of ¹O₂ quantum yield

 $^{1}O_{2}$ quantum yields were determined for solutions containing SOA material, SOA precursor compounds, two reference materials, specifically juglone and Suwannee River fulvic acid, and two ambient PM₁₀ filters (Table S2). Perinaphthenone (PN) was used as a reference $^{1}O_{2}$ sensitizer with a wavelength-independent quantum yield of 0.98 ± 0.08 . The sensitized photolysis experiments were performed in individual borosilicate test tubes using the same irradiation conditions for PN and the test mixtures. $^{1}O_{2}$ quantum yields were calculated according to equation (2):

$$\phi_{1O_2} = \frac{k_{obs}^{SOA}}{k_{obs}^{PN}} \times \frac{R_{abs}^{PN}}{R_{obs}^{SOA}} \times \phi_{PN}$$
(2)

where k_{obs}^{SOA} and k_{obs}^{PN} are the observed degradation rate constants for FFA in the presence of SOA material and PN, R_{abs}^{SOA} and R_{abs}^{PN} are the rates of light absorption for SOA and PN (section 4.1 in SI).

7. Quantification of OH radical steady-state concentrations and quantum yields

 $3 \times 10^{-18} M$.

OH radicals were quantified using the 311 nm light source. According to the method described by Page at al.³³, potassium terephthalate (TPA) was added to the solution and used as an OH radical probe. The reaction of OH radicals with TPA produces hydroxyterephthalate (hTPA), which was monitored over time by UPLC-PDA (Waters ACQUITY). The rate of hTPA production (RhTPA) was measured for seven TPA concentrations, ranging from 20 to 400 µM (Figure S6). The rate was determined using the asymptote of the curve generated from RhTPA plotted against TPA concentration (Figure S6b). The slopes of the curves were multiplied by RoH and by the reaction rate constant of TPA with OH radicals to obtain the OH radical scavenging rate constant of the SOA extracts, k'OH. [OH]_{ss} under conditions of no probe were obtained by dividing ROH by k'OH. The hydroxyl radical steady-state concentrations, [OH]_{ss}, was also determined under conditions of no probe, following the approach described by Zhou and Mopper (section 4.2.1. in SI).³⁴ Under our experimental conditions, the limit of detection of hTPA is 1 × 10⁻⁸ M, which corresponds to a minimum detectable OH radical steady-state concentration of

The OH radical generation quantum yields were determined for all the mixtures described above according to equation (3):

$$\phi_{OH} = R_{OH}/R_{abs} \tag{3}$$

where R_{OH} is the rate of OH radical production and R_{abs} is the rate of light absorption by the solution (section 4.2 in SI).

8. Quantification of hydrogen peroxide production and quantum yield

Hydrogen peroxide production was quantified using the horseradish peroxidase (HRP)-Amplex Red method. A horseradish peroxidase solution was prepared by combining $10 \mu L$ of a 10 mM Amplex Red solution in DMSO, $20 \mu L$ of 10 U/mL horseradish peroxidase solution in 50 mM phosphate buffer pH 7.4, and 1 mL of 50 mM phosphate buffer at pH 7.4. Each sample was irradiated at 311 nm and $50 \mu L$ aliquots were taken every 30 minutes. Then, $50 \mu L$ of the horseradish peroxidase mixture was added to the aliquot. In the presence of the horseradish peroxidase enzyme, Amplex Red reacts quantitatively with H_2O_2 to produce fluorescent resorufin with a yield of $\sim 100\%$. After incubation in darkness for at least 30 min to produce resorufin, the samples were analyzed for resorufin using ultra high-pressure liquid chromatography (UPLC, Waters ACQUITY) coupled with a photodiode array detector (Figure S8). The detection limit of H_2O_2 was $2 \times 10^{-7} M$ under our experimental conditions.

Hydrogen peroxide quantum yields were obtained as the ratio of the hydrogen peroxide production rate, measured with the HRP-Amplex Red method, and the rate of light absorption using equation (4) (Table S6 and section 4.3 in SI).

$$\phi_{H_2O_2} = R_{H_2O_2}/R_{abs} \tag{4}$$

Results and discussion

1. ¹O₂ production from SOA extracts

The filter extracts from toluene, biphenyl, naphthalene and 1,8-dimethylnaphthalene SOA efficiently sensitized ¹O₂ and produced OH radicals as well as peroxides upon irradiation with

single wavelength UVB light at 311 nm. The ¹O₂ steady-state concentrations, measured in these conditions for 5 mg_C L⁻¹ solutions of SOA extracts, ranged between 1.1×10^{-14} and 4.5×10^{-14} M with an average of $(3 \pm 1) \times 10^{-14}$ M (Figure 1). All SOA extracts from aromatic precursors showed ${}^{1}O_{2}$ quantum yields ranging between 1.2×10^{-2} and 3.2×10^{-2} (Table 1). These results show that laboratory-generated anthropogenic SOA material can generate a significant amount of ¹O₂ when irradiated with UV light, an observation currently underappreciated in aerosol ROS chemistry. For comparison, the ¹O₂ quantum yield of Suwannee River fulvic acid (SRFA), a commercially available and well-studied dissolved organic matter within the field of aquatic photochemistry, was 0.034 under identical experimental conditions (Table S2), consistent with the literature range of 0.01-0.04. $^{37-41}$ We can conclude that the $^{1}O_{2}$ quantum yield measured for SOA generated from aromatic precursors, compares well with ¹O₂ quantum yields known for chromophoric dissolved organic matter. In addition, α-pinene SOA was used as a control non-aromatic precursor-generated SOA (Table S1). We did not expect α-pinene SOA to sensitize ¹O₂, since compounds found in this SOA do not contain conjugated double bonds or aromatic systems, and indeed have limited ability to absorb light, as shown by its UV-vis spectra (Figures S1 and S2) and SUVA₂₅₄ (Table S9). As expected, no quantifiable ¹O₂ production could be observed when α-pinene SOA was used as ¹O₂ sensitizer. Furthermore, we conducted ¹O₂ experiments with the pure precursor compounds of the SOA filters (toluene, biphenyl, naphthalene and 1,8-dimethylnaphthalene) in aqueous solutions at a concentration of 5 mg_C L⁻¹. These compounds did not show any ¹O₂ production, except for 1,8dimethylnaphthalene which displayed ¹O₂ sensitizing ability, although much lower than its

208

209

210

211

212

213

214

215

216

217

218

219

220

221

222

223

224

225

226

227

228

229

corresponding SOA material. Specifically, a solution of 1,8-dimethylnaphthalene showed a $^{1}O_{2}$ quantum yield of 0.3×10^{-2} , one order of magnitude smaller than the SOA material prepared by oxidation of 1,8-dimethylnaphthalene (3.2×10^{-2}). This result suggests that photosensitizing moieties are produced during the photooxidation of the SOA precursor compounds inside the smog chamber, which is known for toluene oxidation product. 42,43

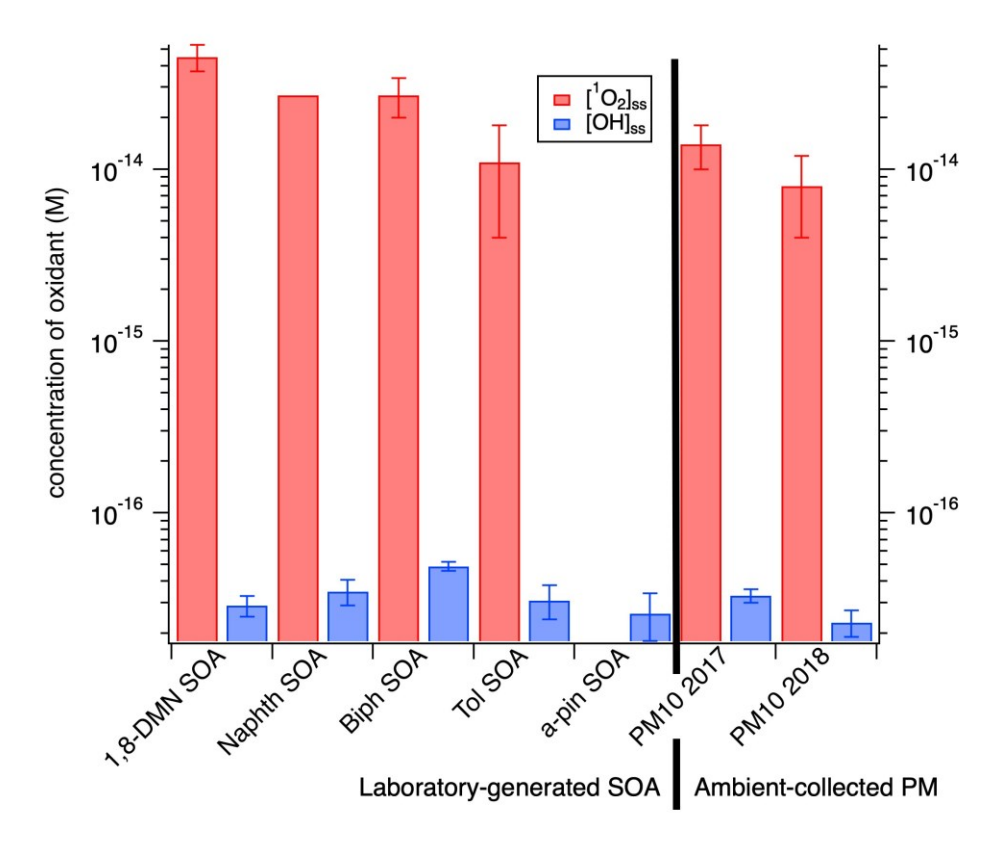


Figure 1: Steady-state concentrations of 1O_2 and OH radicals quantified for irradiation at 311 nm within laboratory-generated SOA and ambient-collected PM $_{10}$ filters. No quantifiable FFA degradation was observed with α -pinene SOA.

2. OH radicals and H_2O_2 production from SOA extracts

In the context of evaluating the relevance of 1O_2 within ROS produced in irradiated SOA and PM_{10} extracts, we also quantified the production of OH radicals and H_2O_2 . All irradiated SOA samples at 311 nm produced steady-state concentrations of hydroxyl radicals between 2.6×10^{-17}

to 4.9×10^{-17} M (Figure 1). Note that these concentrations are three orders of magnitude lower 245 246 than the steady-state concentrations of ${}^{1}O_{2}$, quantified for the same agueous SOA samples. OH radical quantum yields were also calculated and ranged between 4.6×10^{-5} and 6.8×10^{-5} , three 247 orders of magnitude smaller than ¹O₂. 248 249 In addition, biphenyl and 1,8-dimethylnaphthalene SOA extracts were found to have slightly lower quantum yields for producing OH radicals (5.1 \times 10⁻⁵ and 4.6 \times 10⁻⁵ respectively), 250 compared to naphthalene and toluene SOA (6.3×10^{-5}) and 6.8×10^{-5} , respectively) (Table 1 and 251 252 Figure 2). Irradiation of solutions of pure organic compounds that served as SOA precursors 253 (toluene, biphenyl, naphthalene and 1,8-dimethylnaphthalene) did not show any OH radical 254 production under the same experimental conditions. This result further supports that the ability of 255 producing ROS derives from functional groups formed in the aerosol production process. The competition kinetic approach used to determine [OH]_{ss} and OH radical production rates, 256 257 allowed us to estimate the OH radical scavenging rate constant of SOA mixtures and PM₁₀ extracts (k'_{OH}). Values obtained ranged between 3.5 and 8.9 × 10⁻⁵ s⁻¹ (Table S4), similar to 258 dissolved organic matter samples and fog waters by Arakaki et al.⁴⁴ We further calculated the 259 ratio between k'_{OH} and the TOC, finding values between 3.0 and 7.5×10^{-8} L M_C^{-1} s⁻¹ (Table S4), 260 in agreement with previously reported values for dissolved organic matter, 44 fog waters, 44 and 261 particle extracts.¹² 262 Furthermore, all anthropogenic and biogenic SOA samples were able to generate H₂O₂, 263 264 although to a different extent. Since H₂O₂ concentrations increased with irradiation time, no 265 steady-state concentrations can be determined (Figure S6a). Naphthalene, 266 dimethylnaphthalene and α-pinene SOA had similar H₂O₂ quantum yields, while biphenyl and 267 toluene SOA showed a lower activity (Table 1 and Figure 2). As expected, the pure compounds

did not produce H_2O_2 , except for 1,8-dimethylnaphthalene with a quantum yield of 1.5×10^{-4} . The H_2O_2 quantum yields are one order of magnitude larger than the OH radical quantum yields and ranged between 2.5×10^{-4} and 4.5×10^{-4} .

When comparing OH and ${}^{1}O_{2}$ quantum yields and steady-state concentrations, we observed that the OH radical quantum yields and resulting concentrations were three orders of magnitude smaller (Table 1, Figure 2). The higher concentration of ${}^{1}O_{2}$ is balanced by its higher substrate selectivity and lower reactivity,⁴⁵ which make OH radicals and ${}^{1}O_{2}$ competitive oxidants for processing air pollutants and tracers.

In addition, a fraction of the OH radicals are likely generated by H_2O_2 photolysis. If this photolysis is the rate limiting step, which is a reasonable assumption based on H_2O_2 concentrations increasing with time, then one could expect higher quantum yields for H_2O_2 compared to OH radicals.

3. $^{1}O_{2}$, OH radical and $H_{2}O_{2}$ comparison between SOA and PM_{10} extracts

Our results suggest the importance of ${}^{1}O_{2}$ as an oxidant in anthropogenic SOA. Because these aerosols were generated within a smog chamber at high concentrations and may not accurately represent the real atmosphere, we extended our study to two 24 hour-integrated PM₁₀ filters, collected in Graubünden, Switzerland. Irradiated PM₁₀ filter extracts at 311 nm produced ROS (Figure 2 and Table 1). We found that steady-state concentrations of ${}^{1}O_{2}$ were comparable to those for SOA prepared from toluene but lower than for SOA prepared from larger aromatic compounds (Figure 1). On the other hand, they showed systematically higher ${}^{1}O_{2}$ quantum yields than SOA mixtures (Table 1). Their average ${}^{1}O_{2}$ steady-state concentration and production quantum yield were 1.1×10^{-14} M and 0.043 respectively. The sensitizing ability of PM₁₀ extracts further supports the importance of ${}^{1}O_{2}$ in atmospheric processing of organic aerosols.

The PM_{10} samples were also tested for the production of OH radicals and H_2O_2 . OH radical quantum yields were on the same order of magnitude than those for the SOA mixtures, albeit two to three times higher (Table 1, Figure 2). PM_{10} samples also produced H_2O_2 , with quantum yields in the range of 3.9 to 6.5×10^{-4} . These findings indicate that ROS quantum yields measured from the laboratory-generated SOAs are comparable to quantum yields from actual field-collected atmospheric particulate matter.

Table 1. Summary of measured ROS steady-state concentrations and quantum yields for SOA samples and PM_{10} filters, the error reported for $[^{1}O_{2}]_{ss}$ represents the standard deviation of 3 measurements, while the errors reported for quantum yields are propagated errors. No uncertainty is associated with naphthalene SOA because not enough material was collected to repeat at least three measurements.

Entry	$TOC \pmod{Mg_C/L}$	$[^{1}O_{2}]_{ss}$ $(10^{-14} M)$	$\Phi^{1}O_{2}$ (10 ⁻²)	$[OH^{-}]_{ss}$ $(10^{-17} M)$	Φ OH· (10 ⁻⁵)	$\Phi \text{ H}_2\text{O}_2 $ (10^{-4})
1,8-DMN SOA	5	4.5 ± 0.8	3 ± 1	2.9 ± 0.4	4.6 ± 0.9	4.5 ± 0.4
1,8-DMN	5	2.2 ± 0.6	0.3 ± 0.2	< 0.3	nd	1.5 ± 0.6
Naphthalene SOA	5	2.7	2.3	3.5 ± 0.6	6.3 ± 1.0	3.5 ± 0.3
Biphenyl SOA	5	2.7 ± 0.7	2.3 ± 0.7	4.9 ± 0.3	5.1 ± 1.0	2.5 ± 0.2
Toluene SOA	5	1.1 ± 0.7	1.2 ± 0.3	3.1 ± 0.7	6.8 ± 1.3	2.6 ± 0.3
α-pinene SOA	5	< 0.3	nd	2.6 ± 0.8	nd	4.3 ± 0.4
PM ₁₀ filter Nov 2017	5	1.4 ± 0.4	4.5 ± 0.4	3.3 ± 0.3	11 ± 4	3.9 ± 0.6
PM ₁₀ filter Mar 2018	5	0.8 ± 0.4	4.0 ± 0.3	2.3 ± 0.4	24 ± 5	6.5 ± 0.7

nd = not determined

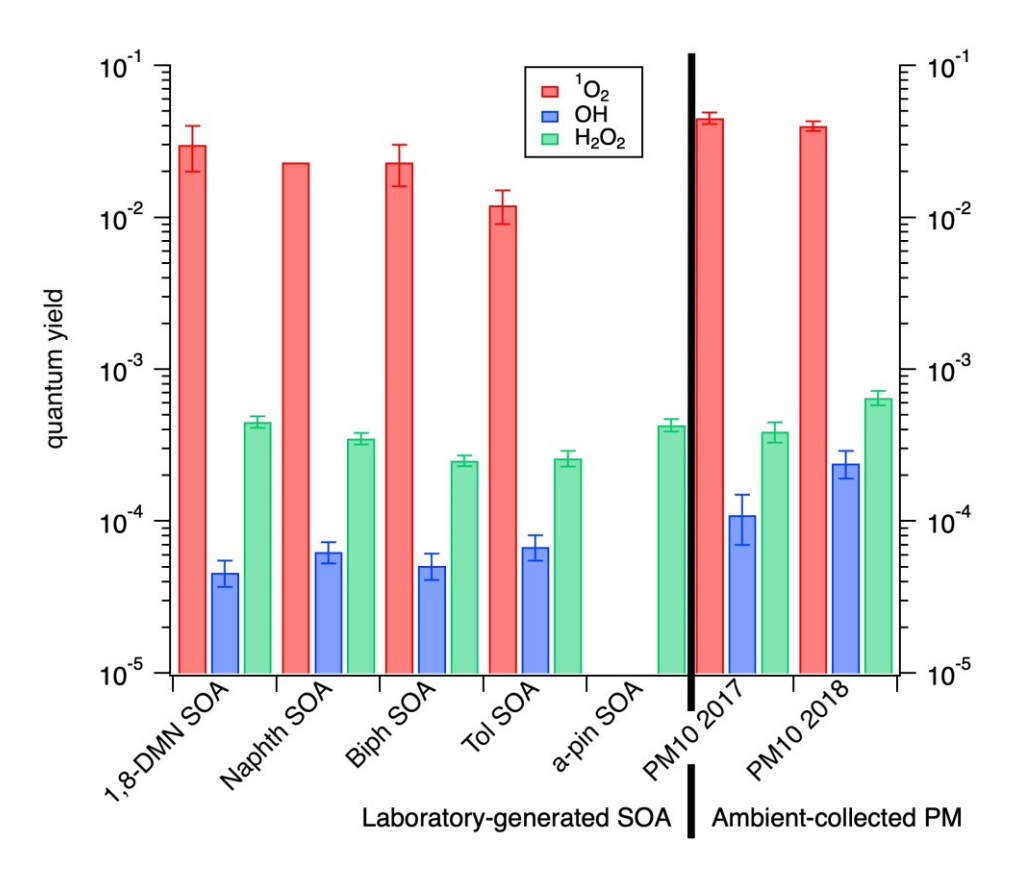


Figure 2: Quantum yields of each oxidant measured at 311 nm for laboratory-generated SOA and ambient-collected PM_{10} .

4. Origin of SOA and PM₁₀ extracts' sensitizing ability

In order to understand the origin of the sensitizing ability of SOA, we evaluated the aromaticity of SOA samples, since it is known that aromatic structures are important light-absorbing moieties and promote the photosensitizing ability of organic compounds. ⁴⁶ The photooxidation of aromatic hydrocarbons can produce compounds with a retained aromatic moiety and compounds with ring-opened and oxidized functionalities. For example, products of oxidation of naphthalene include substituted naphthalene compounds, such as naphthols, as well as substituted benzene compounds, such as hydroxy benzoic acids. ⁴⁷ The gas phase mechanism of toluene oxidation also can similarly lead to phenolic type compounds. ⁴⁸ In this section, we

discuss the specific ultraviolet absorbance at 254 nm (SUVA₂₅₄), the aromaticity equivalent (X_c), and the sensitizing ability of juglone to assess the origin of {}^{1}O_{2} within chromophoric SOA and PM₁₀ extracts.⁴⁹

325

326

327

328

329

330

331

332

333

334

335

336

337

338

339

340

341

342

343

344

322

323

324

4.1. SUVA₂₅₄

The effective aromaticity of toluene, biphenyl, naphthalene, 1,8-dimethylnaphthalene and α pinene SOA samples, as well as PM₁₀ filters, was estimated by calculating the specific ultraviolet absorbance at 254 nm (SUVA₂₅₄), previously used as a proxy for organic matter aromaticity.⁵⁰ The SUVA₂₅₄, calculated by normalizing the absorbance at 254 nm with the total organic carbon of the mixture, ranged between 2.0 and 4.5 L mg_C⁻¹ m⁻¹, showing appreciable aromatic content in aromatic SOA extracts and PM₁₀ filters (Table S9). The highest SUVA₂₅₄ value was found for biphenyl SOA, likely due to the presence of two independent aromatic structures capable of preserving aromaticity during photooxidation.⁵¹ α-pinene SOA had a low SUVA₂₅₄ value of 0.3, consistent with the absence of aromatic structures in the mixture (Table S9). PM₁₀ filters had reduced SUVA₂₅₄ values compare to SOA materials, agreeing with their lower ¹O₂ steady-state concentrations and thus with their higher quantum yields. The same effect was previously noted in fractionated dissolved organic matter, where less aromatic fractions showed higher quantum yields due to their limited rate of light absorption. 41,52 In addition, we found a correlation between the rate of light absorption at 311 nm and the ¹O₂ steady-state concentrations with SUVA₂₅₄ values, suggesting that an increase in aromatic content produces higher rates of light absorption and therefore higher ¹O₂ steady-state concentrations (Figure 3). SUVA₂₅₄ values were also estimated after 4 hours of irradiation at 311 nm and 365 nm, showing no significant change in the absorption of the mixtures (Figure S9).

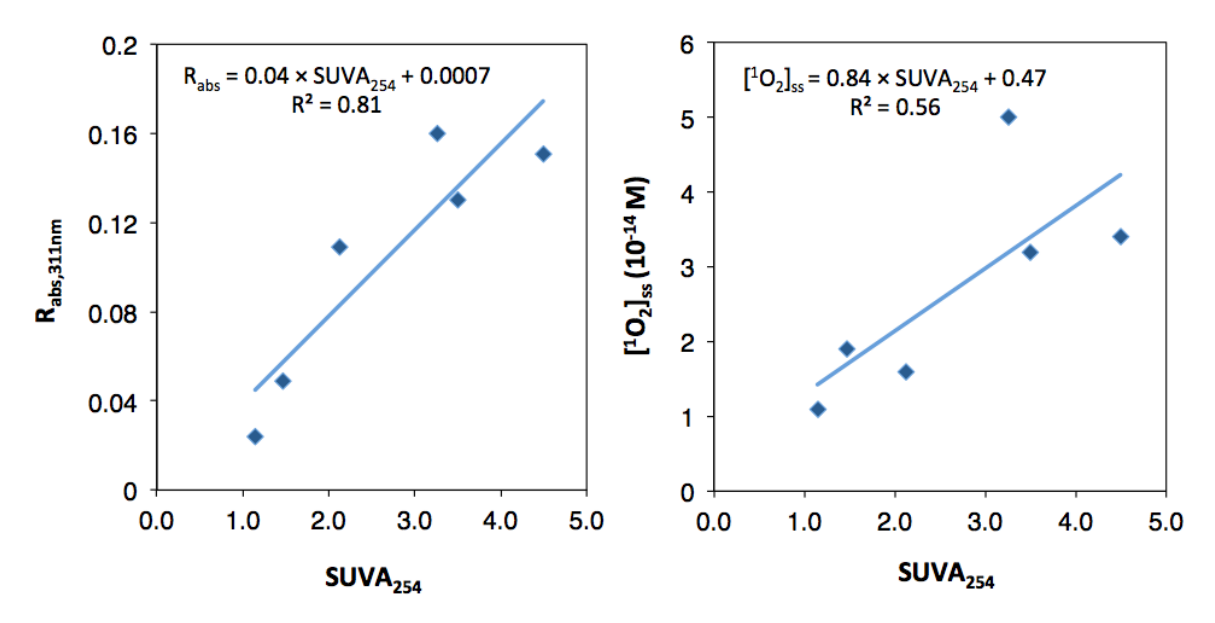


Figure 3: Left: Correlation plot of the rate of absorbance at 311 nm of SOA samples and PM_{10} filters (total of six extracts) as a function of SUVA at 254 nm. Right: Correlation plot of ${}^{1}O_{2}$ steady-state concentrations of the same six extracts as a function of SUVA₂₅₄.

4.2. Aromaticity equivalent

High resolution mass spectrometry (HRMS) analysis (section 6 of SI) of the SOA samples were performed, and yielded mass spectra of a complex mixture of oxidized organic compounds, with masses up to 350 Da (Figure S10). We calculated the aromaticity equivalent values (X_c) from assigned molecular formulas (Figure S11).⁴⁹ For aromatic SOA materials, X_c values were \geq 2.5, representative of the threshold for the presence of aromatics and condensed aromatics in the mixture.⁴⁹ The X_c values were calculated at 0 and at 4 hours of irradiation for toluene, biphenyl, naphthalene and 1,8-dimethylnaphthalene SOA extracts, as well as for PM₁₀ extracts. As for the SUVA₂₅₄ values, we observed no significant changes in X_c values after 4 hours of irradiation (Figure S11), indicating no depletion in the aromatic content of the mixtures. This evidence is in good agreement with the constant rate of FFA degradation over time, implying a steady-state concentration of ${}^{1}O_{2}$ when SOA samples are irradiated over the timescale of 4 hours. Since the

¹O₂ sensitizing ability of SOA is not measurably depleted during irradiation, we suggest that the ROS produced do not modify the sensitizing properties within our experimental timescales. We also plotted for the four SOA extracts the H/C vs O/C ratios (Figure S12), the nominal carbon oxidation state vs carbon number (Figure S13) and aromaticity index vs carbon number (Figure S14), all with the same conclusion.

4.3. Juglone as a sensitizer

We identified a peak at m/z of 174.0321 in naphthalene SOA, which we tentatively assigned to juglone, a hydroxy-benzoquinone known as a naphthalene oxidation intermediate.⁵³ We tested the ability of juglone to produce ${}^{1}O_{2}$, and measured a ${}^{1}O_{2}$ steady-state concentration of 7.5×10^{-14} M and a quantum yield of 0.11 (Table S2). The ${}^{1}O_{2}$ steady-state concentration of juglone fell in the range of the measured SOA extracts. The quantum yield of juglone was higher than the quantum yield of the SOA extracts since, as a pure compound, it did not absorb as much light as organic matter without sensitizing ${}^{1}O_{2}$. This observation is consistent with our hypothesis that the presence of aromatics is important for sensitizing ${}^{1}O_{2}$. Yet, if 1,4-quinone moieties were the major sensitizing moiety, a difference between the ${}^{1}O_{2}$ concentrations of naphthalene and 1,8-dimethylnaphthalene would have been observed, since 1,8-dimethylnaphthalene cannot form 1,4 quinones. Since this difference was not observed, we can only state that aromatic quinones, such as juglone, are likely one of many classes of ${}^{1}O_{2}$ sensitizers in SOA derived from aromatic precursors.

5. Comparison of ¹O₂ and OH radical quantum yields with the literature

To place our findings in the context of different aerosol types and understand the importance of SOA-produced ROS in the oxidation of air pollutants and particulate matter, we compare our

ROS quantum yields with previously published measurements of fog, rain and cloud waters as well as road dust (Table 2). Faust and Allen reported the first measurement of $^{1}\mathrm{O}_{2}$ steady-state concentration in cloud water, ¹⁶ with values comparable to this work for SOA and PM₁₀ extracts. However, the reported quantum yields span a wider range, likely due to the variability of the sampling locations. Anastasio and McGregor measured ¹O₂ and OH radical steady-state concentrations in fog waters, 18 using the same FFA method employed in this study, and reported 4 to 20 times higher concentrations, but comparable OH radical quantum yields. Albinet and Vione measured 1O2 and OH radical steady-state concentrations in rain water and detected no ¹O₂, but a high concentration of OH radicals. ¹⁹ Kaur and Anastasio measured the same oxidants in fog water samples collected in Davis, California, ¹⁷ finding an average ¹O₂ quantum yield of 4.2×10^{-2} , which compares well with our SOA and PM₁₀ extracts. In addition, the OH radical quantum yields reported for fog waters were six times larger than for our SOA extracts. This difference could potentially be ascribed to the presence of fewer OH radical sources in SOA than in fog water. Kaur and Anastasio indeed reported that 70% of the OH radical production was due to NO₂ and NO₃ in fog waters, while these anions are not present in our SOA extracts. Furthermore, Cote et al. reported the ¹O₂ production from aqueous road dust and showed that irradiated extracts generated ¹O₂ with steady-state concentrations of 1×10⁻¹³ M, ²⁰ however ¹O₂ quantum yields were not reported and therefore experimental conditions cannot be directly compared at this time. Most recently, Kaur et al. quantified ¹O₂, OH radicals and triplet state organic matter within fog and particulate matter in Davis, California. ¹² They obtained higher ¹O₂ steady-state concentrations, in agreement with their use of 50% D₂O as a solvent, which extends ¹O₂ lifetime by a factor of 2, and their use of a xenon lamp.

407

385

386

387

388

389

390

391

392

393

394

395

396

397

398

399

400

401

402

403

404

405

Table 2. Summary of singlet oxygen and hydroxyl radical steady-state concentrations and quantum yields for atmospherically relevant aqueous solutions. The values are reported as ranges, note that steady-state concentrations are dependent on the TOC of the sample and the illumination method.

Material	$[^{1}O_{2}]_{ss}$	•	[OH ⁻] _{ss} (10 ⁻¹⁷ M)	•	Reference	
<u></u>			(10 101)	(10)		
Cloud water	$2.7 - 110^{a}$	4.8 - 20			Faust et al., J. Geophys. Res.	
					1992	
Fog water	$11 - 61^{b}$		$17 - 77^{b}$	1 - 64	Anastasio & McGregor,	
					Atmos. Environ. 2001	
Rain water	\leq 0.27 $^{\rm c}$		87 – 150 ^c		Albinet & Vione, Sci. Total	
					Environ. 2010	
Fog water	$1.1 - 30^{b}$	1.1 – 12	26 – 110 ^b	15 - 87	Kaur et al., Atmos. Environ.	
					2017	
Road dust	$0.83 - 10^{d}$				Cote et al., Environ. Sci.	
extracts					Technol. Lett. 2018	
PM ₁₀ extracts	$6.4 - 220^{e}$	2.2 - 5.7	17 – 79 ^e	6.2 - 35	Kaur et al., Atmos. Chem.	
					Phys. 2019	
SOA extracts	$1.1 - 4.5^{\ f}$	1.2 - 3	$2.6 - 4.9^{\ f}$	4.6 – 6.8	This work	
PM ₁₀ extracts	$0.8 - 1.4^{\mathrm{f}}$	4.0 – 4.5	$2.2 - 3.3^{\ f}$	11 – 24	This work	

413 ^a Midday, equinox-normalized steady-state concentration

^b Winter solstice-normalized steady-state concentration

415 c Values obtained with UV-A lamps at 365 nm with a photon flux of 1.6×10^{-5} E L⁻¹ s⁻¹

^d Steady-state concentration obtained by irradiation with a solar simulator

^e Steady-state concentration measured in D₂O irradiating with a xenon arc lamp

^fSteady-state concentration obtained by irradiation at 311 nm

Atmospheric implications

421

422

423

424

425

426

427

428

429

430

431

432

433

434

435

436

437

438

439

440

441

442

443

420

In this work, we tested and verified the hypothesis that SOA generated from aromatic compounds are capable of photosensitizing ¹O₂. The measured concentrations of ¹O₂ were three orders of magnitude higher than those of OH radical, indicating that ¹O₂ could play a role in oxidizing air pollutants and tracers. To compare the relevance of these two oxidants for the fate of environmentally relevant pollutants and air tracers, we performed a kinetic box model for organic compounds with known ¹O₂ and OH radical reaction rate constants (Figure 4, Table S9). The goal is to highlight the potential of ${}^{1}O_{2}$ as a relatively important oxidant in organic aerosol processing. For ¹O₂ and OH radical steady-state concentrations, we used the average values from our SOA measurements of 3×10^{-14} M and 4×10^{-17} M, respectively, and we used literature reaction rate constants for the following organic compounds: benzimidazole, 4-nitrophenol, imidazole, indole, syringol, histidine, resorcinol, niclosamide, tryptophan, vanillin, hydroquinone, methionine, tyrosine and cysteine. 54-70 Some of these compounds are potentially found in atmospheric aerosols, such as benzimidazole, cysteine⁷¹, nitrophenols^{72,73}, tyrosine⁷¹, syringol and vanillin^{74,75}. We opted not to consider H₂O₂ as part of this box model because of its low concentrations and low reactivity with organics compared to the other two ROS. The 14 compounds studied here could be classified into two categories: overall lifetimes against ROS reduced by (1) more than 50% and by (2) less than 50%, when including ¹O₂ as a sink (Figure 4). In general, the lifetime of compounds which contain electron-rich aromatic rings such as histidine, imidazole, resorcinol, indole, tryptophan and hydroquinone is strongly affected by the presence of ${}^{1}O_{2}$ (Figure 4). Of note, histidine's lifetime against OH is 59 days, whereas its lifetime against OH radicals and ${}^{1}O_{2}$ is 4 days, indicating that ${}^{1}O_{2}$ is the major sink for histidine in proteinaceous aqueous aerosols. Furthermore, other amino acids (e.g. tryptophan, methionine),

organo-nitrogen compounds (imidazole, indole, niclosamide) and phenolic compounds (hydroquinone, resorcinol) have shortened lifetimes by more than a factor of two when ¹O₂ reactivity is considered in their overall fate (Figure 4). On the other hand, the second category of compounds with lifetimes affected to a lesser extent by ¹O₂ reactivity also include amino acids and phenolic compounds, and thus it remains difficult to predict on a single compound basis the effect of an additional sink against ¹O₂. To further corroborate the importance of ${}^{1}O_{2}$ as a potential atmospheric oxidant for organic aerosol processing, Kaur et al. recently came to the same conclusion when looking at the contributions of OH radicals, ¹O₂ and triplet state organic carbon to PM and fog water processing. 12 Therefore, the omission of 1O2 reactivity in SOA processing models could lead to the overestimation of the lifetimes of aromatic pollutants and atmospheric aerosol tracers. We also recommend that ¹O₂ rate coefficients with key atmospheric pollutants be the focus of further organic aerosol kinetics research. It is also likely that ¹O₂ is participating in atmospheric aging of organic aerosols.⁷⁶ From the results reported in this work, it is clear that irradiated aromatic SOA can produce ROS, including ¹O₂, in the atmosphere. In the literature, photochemical processing of organic aerosols has been primarily attributed to OH radicals from organic peroxide decomposition and Fenton chemistry, 77 but it is likely that ${}^{1}O_{2}$ is also participating in the same photochemical processing, and play an important role in the oxidation of certain air pollutants. ¹O₂ is a selective oxidant and typically shows reaction rate constants with organic molecules 2 to 3 orders of magnitude smaller than OH radical, however, the measured ¹O₂ steady-state concentrations here and in other recent publications are about 3 orders of magnitude larger than OH radical (see Table 2). Consequently, we expect ¹O₂ to be a competitive oxidant to OH radicals.

444

445

446

447

448

449

450

451

452

453

454

455

456

457

458

459

460

461

462

463

464

465

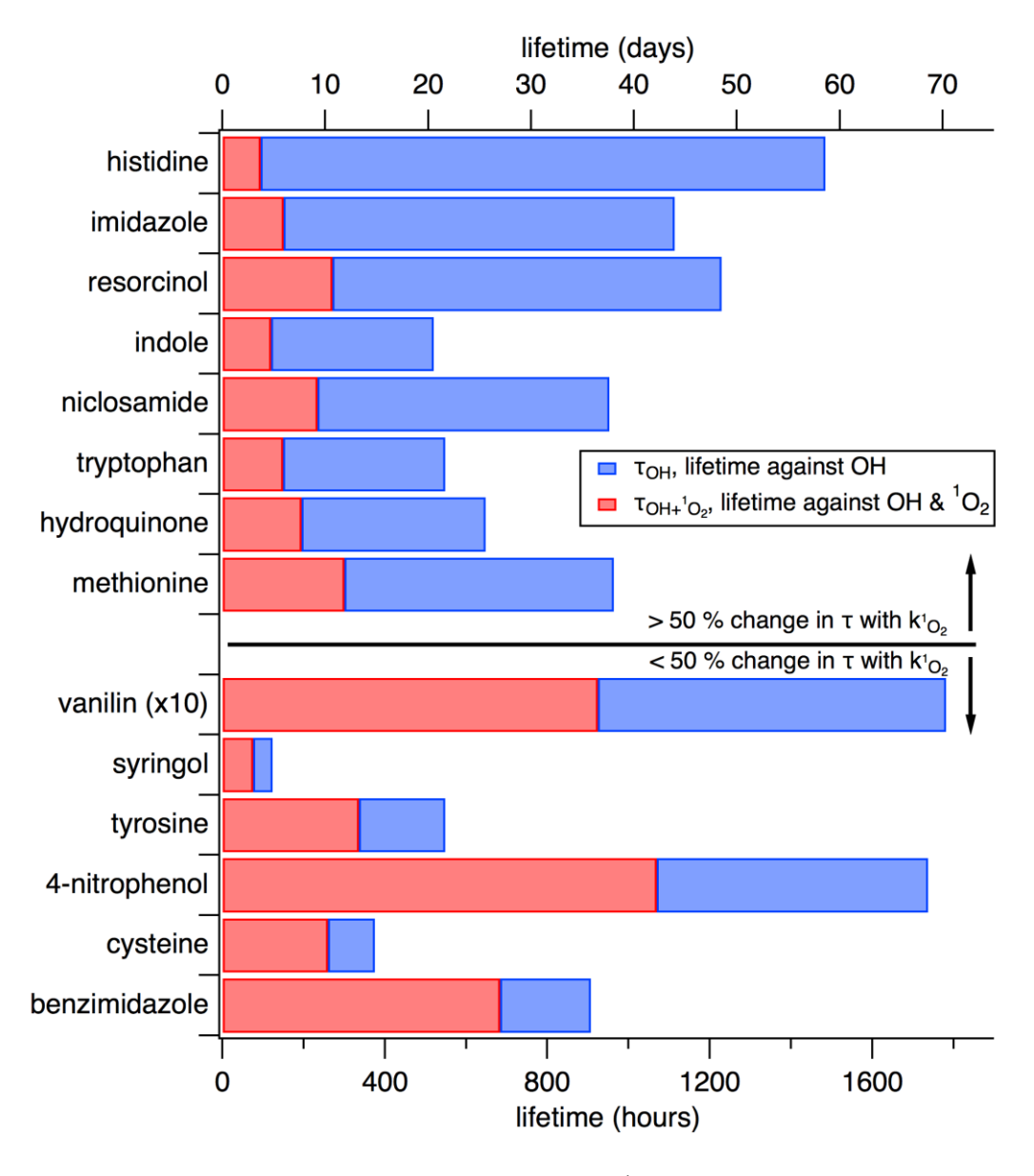


Figure 4: Results of a kinetic box model for ${}^{1}O_{2}$ and OH radical contribution to the environmental lifetimes of selected tracers. The 14 compounds were selected because they have known OH radical and ${}^{1}O_{2}$ reaction rate constants in water. In addition, the compounds were categorized into two categories depending on whether their overall lifetime was affected by more or by less than 50% with the consideration of ${}^{1}O_{2}$ as sink.

475 ASSOCIATED CONTENT

476	Supporting Information. UV-vis spectra of SOA samples, quantum yields calculations for SOA,
477	SRFA, juglone, PM_{10} filters and precursor compounds, rate constants used in the model box calculation,
478	SUVA ₂₅₄ , MS data.
479	
480	AUTHOR INFORMATION
481	Corresponding Author
482	*Nadine Borduas-Dedekind, nadine.borduas@usys.ethz.ch
483	Institute of Biogeochemistry and Pollutant Dynamics
484	ETH Zürich, CHN O 16.2
485	Universitätstrasse 16
486	8092 Zürich
487	Phone: +41 44 632 7315
488	E-Mail: nadine.borduas@usys.ethz.ch
489	Twitter: @nadineborduas
490	Author Contributions
491	The manuscript was written through contributions of all authors. All authors have given approval
492	to the final version of the manuscript.
493	Funding Sources
494	We acknowledge the Swiss National Science Foundation (Grant no. 200020_159809) and SNSF
495	Ambizione Grant (PZ00P2_179703) as well as the American National Science Foundation (NSF)
496	through the Graduate Research Fellowship Program and NSF grant AGS-1853639.
497	ACKNOWLEDGMENT
498	The authors would like to thank Jeroen van den Wildenberg for his technical help and Rachele
499	Ossola for helpful discussions. We also acknowledge Dr. Kyle Moor for wavelength dependence
500	quantum yield discussions and Prof. Christy Remucal for mass spectrometry discussions. We
501	further thank the anonymous reviewers for insightful suggestions.
502	ABBREVIATIONS

- 503 FFA furfuryl alcohol
- 504 SOA secondary organic aerosol
- 505 TOC total organic carbon
- 506 NPOC non-purgeable organic carbon
- 507 ROS reactive oxygen species
- 508 SRFA Suwannee River fulvic acid

510 REFERENCES

- 511 (1) Jimenez, J. L.; Canagaratna, M. R.; Donahue, N. M.; Prevot, A. S. H.; Zhang, Q.; Kroll, J. H.; DeCarlo, P. F.; Allan, J. D.; Coe, H.; Ng, N. L.; Evolution of Organic Aerosols in the Atmosphere. *Science* **2009**, *326* (5959), 1525–1529.
- 514 (2) George, C.; D'Anna, B.; Herrmann, H.; Weller, C.; Vaida, V.; Donaldson, D. J.; Bartels-515 Rausch, T.; Ammann, M. Emerging Areas in Atmospheric Photochemistry. In 516 Atmospheric and Aerosol Chemistry; McNeill, V. F., Ariya, P. A., Eds.; Topics in Current 517 Chemistry; Springer Berlin Heidelberg, 2012; pp 1–53.
- 518 (3) Jokinen, T.; Kontkanen, J.; Lehtipalo, K.; Manninen, H. E.; Aalto, J.; Porcar-Castell, A.; 519 Garmash, O.; Nieminen, T.; Ehn, M.; Kangasluoma, J.; Solar Eclipse Demonstrating the Importance of Photochemistry in New Particle Formation. *Sci. Rep.* **2017**, *7*, 45707.
- 521 (4) George, C.; Ammann, M.; D'Anna, B.; Donaldson, D. J.; Nizkorodov, S. A. Heterogeneous 522 Photochemistry in the Atmosphere. *Chem. Rev. Wash. DC U. S.* **2015**, *115* (10), 4218– 523 4258.
- 524 (5) George, I. J.; Slowik, J.; Abbatt, J. P. D. Chemical Aging of Ambient Organic Aerosol from 525 Heterogeneous Reaction with Hydroxyl Radicals. *Geophys. Res. Lett.* **2008**, *35* (13), 4218-526 4258.
- 527 (6) Cruz, C. N.; Pandis, S. N. Deliquescence and Hygroscopic Growth of Mixed 528 Inorganic-Organic Atmospheric Aerosol. *Environ. Sci. Technol.* **2000**, *34* (20), 4313– 529 4319.
- 530 (7) Freney, E. J.; Adachi, K.; Buseck, P. R. Internally Mixed Atmospheric Aerosol Particles: Hygroscopic Growth and Light Scattering. *J. Geophys. Res.* **2010**, *115*, D19210.
- 532 (8) Laskin, A.; Laskin, J.; Nizkorodov, S. A. Chemistry of Atmospheric Brown Carbon. *Chem. Rev.* **2015**, *115* (10), 4335–4382.
- 534 (9) Ervens, B. Modeling the Processing of Aerosol and Trace Gases in Clouds and Fogs. *Chem.* 535 *Rev.* **2015**, *115* (10), 4157–4198.
- 536 (10) Herrmann, H. Kinetics of Aqueous Phase Reactions Relevant for Atmospheric Chemistry. *Chem. Rev.* **2003**, *103* (12), 4691–4716.
- 538 (11) Herrmann, H.; Schaefer, T.; Tilgner, A.; Styler, S. A.; Weller, C.; Teich, M.; Otto, T. 539 Tropospheric Aqueous-Phase Chemistry: Kinetics, Mechanisms, and Its Coupling to a 540 Changing Gas Phase. *Chem. Rev.* **2015**, *115* (10), 4259–4334.
- 541 (12) Kaur, R.; Labins, J. R.; Helbock, S. S.; Jiang, W.; Bein, K. J.; Zhang, Q.; Anastasio, C. 542 Photooxidants from Brown Carbon and Other Chromophores in Illuminated Particle 543 Extracts. *Atmospheric Chem. Phys.* **2019**, *19* (9), 6579–6594.

- 544 (13) McNeill, K.; Canonica, S. Triplet State Dissolved Organic Matter in Aquatic 545 Photochemistry: Reaction Mechanisms, Substrate Scope, and Photophysical Properties. 546 Environ. Sci. Process. Impacts 2016, 18 (11), 1381–1399.
- 547 (14) Kaur, R.; Anastasio, C. First Measurements of Organic Triplet Excited States in Atmospheric Waters. *Environ. Sci. Technol.* **2018**, *52* (9), 5218–5226.
- 549 (15) Kaur, R.; Hudson, B. M.; Draper, J.; Tantillo, D. J.; Anastasio, C. Aqueous Reactions of 550 Organic Triplet Excited States with Atmospheric Alkenes. *Atmospheric Chem. Phys.* 551 **2019**, 19 (7), 5021–5032.
- 552 (16) Faust, B. C.; Allen, J. M. Aqueous-Phase Photochemical Sources of Peroxyl Radicals and Singlet Molecular Oxygen in Clouds and Fog. *J. Geophys. Res. Atmospheres* **1992**, *97* (D12), 12913–12926.
- 555 (17) Kaur, R.; Anastasio, C. Light Absorption and the Photoformation of Hydroxyl Radical and Singlet Oxygen in Fog Waters. *Atmos. Environ.* **2017**, *164*, 387–397.

558559

563

564

565

566

567568

569

570

571

572

573

574

575

- (18) Anastasio, C.; McGregor, K. G. Chemistry of Fog Waters in California's Central Valley: 1. In Situ Photoformation of Hydroxyl Radical and Singlet Molecular Oxygen. *Atmos. Environ.* **2001**, *35* (6), 1079–1089.
- 560 (19) Albinet, A.; Minero, C.; Vione, D. Photochemical Generation of Reactive Species upon 561 Irradiation of Rainwater: Negligible Photoactivity of Dissolved Organic Matter. *Sci. Total* 562 *Environ.* **2010**, *408* (16), 3367–3373.
 - (20) Cote, C. D.; Schneider, S. R.; Lyu, M.; Gao, S.; Gan, L.; Holod, A. J.; Chou, T. H. H.; Styler, S. A. Photochemical Production of Singlet Oxygen by Urban Road Dust. *Environ. Sci. Technol. Lett.* **2018**, *5* (2), 92–97.
 - (21) Chen, J.; Valsaraj, K. T. Uptake and UV-Photooxidation of Gas-Phase Polyaromatic Hydrocarbons on the Surface of Atmospheric Water Films. 2. Effects of Dissolved Surfactants on Naphthalene Photooxidation. *J. Phys. Chem. A* **2007**, *111* (20), 4289–4296.
 - (22) Richards-Henderson, N.; Pham, A. T.; Kirk, B. B.; Anastasio, C. Secondary Organic Aerosol from Aqueous Reactions of Green Leaf Volatiles with Organic Triplet Excited States and Singlet Molecular Oxygen. *Environ. Sci. Technol.* **2015**, *49* (1), 268–276.
 - (23) Di Mascio, P.; Martinez, G. R.; Miyamoto, S.; Ronsein, G. E.; Medeiros, M. H. G.; Cadet, J. Singlet Molecular Oxygen Reactions with Nucleic Acids, Lipids, and Proteins. *Chem. Rev.* **2019**, *119* (3), 2043–2086.
 - (24) Moan, J.; Berg, K. Photochemotherapy of Cancer: Experimental Research. *Photochem. Photobiol.* **1992**, *55* (6), 931–948.
- 577 (25) Yamazaki, S.; Ozawa, N.; Hiratsuka, A.; Watabe, T. Photogeneration of 3β-Hydroxy-5α 578 Cholest-6-Ene-5-Hydroperoxide in Rat Skin: Evidence for Occurrence of Singlet Oxygen
 579 in Vivo. *Free Radic. Biol. Med.* 1999, 27 (3), 301–308.
- 580 (26) Devasagayam, T. P. A.; Kamat, J. P. Biological Significance of Singlet Oxygen. *Indian J. Exp. Biol.* **2002**, *40* (6), 680–692.
- 582 (27) Malecha, K. T.; Nizkorodov, S. A. Photodegradation of Secondary Organic Aerosol 583 Particles as a Source of Small, Oxygenated Volatile Organic Compounds. *Environ. Sci.* 584 *Technol.* **2016**, *50* (18), 9990–9997.
- 585 (28) Appiani, E.; Ossola, R.; Latch, D. E.; Erickson, P. R.; McNeill, K. Aqueous Singlet Oxygen 586 Reaction Kinetics of Furfuryl Alcohol: Effect of Temperature, pH, and Salt Content. 587 Environ. Sci. Process. Impacts 2017, 19 (4), 507–516.
- 588 (29) Cook, R. D.; Lin, Y.-H.; Peng, Z.; Boone, E.; Chu, R. K.; Dukett, J. E.; Gunsch, M. J.; Zhang, W.; Tolic, N.; Laskin, A.; et al. Biogenic, Urban, and Wildfire Influences on the

- Molecular Composition of Dissolved Organic Compounds in Cloud Water. *Atmospheric Chem. Phys.* **2017**, *17* (24), 15167–15180.
- 592 (30) Buxton, G. V.; Greenstock, C. L.; Helman, W. P.; Ross, A. B. Critical Review of Rate 593 Constants for Reactions of Hydrated Electrons, Hydrogen Atoms and Hydroxyl Radicals 594 (·OH/·O ¯ in Aqueous Solution. *J. Phys. Chem. Ref. Data* **1988**, *17* (2), 513–886.
- 595 (31) Davis, C. A.; McNeill, K.; Janssen, E. M.-L. Non-Singlet Oxygen Kinetic Solvent Isotope 596 Effects in Aquatic Photochemistry. *Environ. Sci. Technol.* **2018**, *52* (17), 9908–9916.
- (32) Schmidt, R.; Tanielian, C.; Dunsbach, R.; Wolff, C. Phenalenone, a Universal Reference
 Compound for the Determination of Quantum Yields of Singlet Oxygen O2(1Δg)
 Sensitization. J. Photochem. Photobiol. Chem. 1994, 79 (1), 11–17.
- 600 (33) Page, S. E.; Arnold, W. A.; McNeill, K. Terephthalate as a Probe for Photochemically Generated Hydroxyl Radical. *J. Environ. Monit.* **2010**, *12* (9), 1658.
- 602 (34) Zhou, X.; Mopper, K. Determination of Photochemically Produced Hydroxyl Radicals in Seawater and Freshwater. *Mar. Chem.* **1990**, *30*, 71–88.
- 604 (35) Towne, V.; Will, M.; Oswald, B.; Zhao, Q. Complexities in Horseradish Peroxidase-605 Catalyzed Oxidation of Dihydroxyphenoxazine Derivatives: Appropriate Ranges for pH 606 Values and Hydrogen Peroxide Concentrations in Quantitative Analysis. *Anal. Biochem.* 607 **2004**, *334* (2), 290–296.
 - (36) Zhao, B.; Summers, F. A.; Mason, R. P. Photooxidation of Amplex Red to Resorufin: Implications of Exposing the Amplex Red Assay to Light. *Free Radic. Biol. Med.* **2012**, 53 (5), 1080–1087.
- 611 (37) Sharpless, C. M. Lifetimes of Triplet Dissolved Natural Organic Matter (DOM) and the 612 Effect of NaBH₄ Reduction on Singlet Oxygen Quantum Yields: Implications for DOM 613 Photophysics. *Environ. Sci. Technol.* **2012**, *46* (8), 4466–4473.

609

- 614 (38) Haag, W. R.; Hoigne, Juerg. Singlet Oxygen in Surface Waters. 3. Photochemical 615 Formation and Steady-State Concentrations in Various Types of Waters. *Environ. Sci.* 616 *Technol.* **1986**, *20* (4), 341–348.
- (39) Marchisio, A.; Minella, M.; Maurino, V.; Minero, C.; Vione, D. Photogeneration of
 Reactive Transient Species upon Irradiation of Natural Water Samples: Formation
 Quantum Yields in Different Spectral Intervals, and Implications for the Photochemistry
 of Surface Waters. Water Res. 2015, 73, 145–156.
- (40) Zepp, R. G.; Schlotzhauer, P. F.; Sink, R. Merritt. Photosensitized Transformations
 Involving Electronic Energy Transfer in Natural Waters: Role of Humic Substances.
 Environ. Sci. Technol. 1985, 19 (1), 74–81.
- 624 (41) Maizel, A. C.; Remucal, C. K. Molecular Composition and Photochemical Reactivity of 625 Size-Fractionated Dissolved Organic Matter. *Environ. Sci. Technol.* **2017**, *51* (4), 2113– 626 2123.
- (42) Lin, P.; Liu, J.; Shilling, J. E.; Kathmann, S. M.; Laskin, J.; Laskin, A. Molecular
 Characterization of Brown Carbon (BrC) Chromophores in Secondary Organic Aerosol
 Generated from Photo-Oxidation of Toluene. *Phys. Chem. Chem. Phys.* 2015, 17 (36),
 23312–23325.
- 631 (43) Jiang, H.; Jang, M.; Sabo-Attwood, T.; Robinson, S. E. Oxidative Potential of Secondary 632 Organic Aerosols Produced from Photooxidation of Different Hydrocarbons Using 633 Outdoor Chamber under Ambient Sunlight. *Atmos. Environ.* **2016**, *131*, 382–389.
- 634 (44) Arakaki, T.; Anastasio, C.; Kuroki, Y.; Nakajima, H.; Okada, K.; Kotani, Y.; Handa, D.; Azechi, S.; Kimura, T.; Tsuhako, A.; et al. A General Scavenging Rate Constant for

- Reaction of Hydroxyl Radical with Organic Carbon in Atmospheric Waters. *Environ. Sci. Technol.* **2013**, *47* (15), 8196–8203.
- (45) Foote, C. S.; Clennan, E. L. Properties and Reactions of Singlet Dioxygen. In *Active Oxygen in Chemistry*; Foote, C. S., Valentine, J. S., Greenberg, A., Liebman, J. F., Eds.;
 Structure Energetics and Reactivity in Chemistry Series (SEARCH Series); Springer Netherlands: Dordrecht, 1995; pp 105–140.
- (46) Aiona, P. K.; Luek, J. L.; Timko, S. A.; Powers, L. C.; Gonsior, M.; Nizkorodov, S. A.
 Effect of Photolysis on Absorption and Fluorescence Spectra of Light-Absorbing
 Secondary Organic Aerosols. ACS Earth Space Chem. 2018, 2 (3), 235–245.

646

647

648

652653

654

- (47) Kautzman, K. E.; Surratt, J. D.; Chan, M. N.; Chan, A. W. H.; Hersey, S. P.; Chhabra, P. S.; Dalleska, N. F.; Wennberg, P. O.; Flagan, R. C.; Seinfeld, J. H. Chemical Composition of Gas- and Aerosol-Phase Products from the Photooxidation of Naphthalene. *J. Phys. Chem. A* **2010**, *114* (2), 913–934.
- (48) Ji, Y.; Zhao, J.; Terazono, H.; Misawa, K.; Levitt, N. P.; Li, Y.; Lin, Y.; Peng, J.; Wang, Y.;
 Duan, L.; et al. Reassessing the Atmospheric Oxidation Mechanism of Toluene. *Proc. Natl. Acad. Sci.* 2017, 114 (31), 8169–8174.
 - (49) Yassine, M. M.; Harir, M.; Dabek-Zlotorzynska, E.; Schmitt-Kopplin, P. Structural Characterization of Organic Aerosol Using Fourier Transform Ion Cyclotron Resonance Mass Spectrometry: Aromaticity Equivalent Approach: Characterization of Organic Aerosol Using FTICRMS. *Rapid Commun. Mass Spectrom.* **2014**, *28* (22), 2445–2454.
- (50) Weishaar, J. L.; Aiken, G. R.; Bergamaschi, B. A.; Fram, M. S.; Fujii, R.; Mopper, K.
 Evaluation of Specific Ultraviolet Absorbance as an Indicator of the Chemical
 Composition and Reactivity of Dissolved Organic Carbon. *Environ. Sci. Technol.* 2003, 37
 (20), 4702–4708.
- (51) Haynes, J. P.; Miller, K. E.; Majestic, B. J. Investigation into Photoinduced Auto-Oxidation
 of Polycyclic Aromatic Hydrocarbons Resulting in Brown Carbon Production. *Environ. Sci. Technol.* 2019, 53 (2), 682–691.
- (52) Rosado-Lausell, S. L.; Wang, H.; Gutiérrez, L.; Romero-Maraccini, O. C.; Niu, X.-Z.; Gin,
 K. Y. H.; Croué, J.-P.; Nguyen, T. H. Roles of Singlet Oxygen and Triplet Excited State of
 Dissolved Organic Matter Formed by Different Organic Matters in Bacteriophage MS2
 Inactivation. Water Res. 2013, 47 (14), 4869–4879.
- 667 (53) McWhinney, R. D.; Zhou, S.; Abbatt, J. P. D. Naphthalene SOA: Redox Activity and Naphthoquinone Gas–Particle Partitioning. *Atmospheric Chem. Phys.* **2013**, *13* (19), 9731–9744.
- (54) Escalada, J. P.; Pajares, A.; Gianotti, J.; Massad, W. A.; Bertolotti, S.; Amat-Guerri, F.;
 García, N. A. Dye-Sensitized Photodegradation of the Fungicide Carbendazim and
 Related Benzimidazoles. *Chemosphere* 2006, 65 (2), 237–244.
- 673 (55) Abdelraheem, W. H. M.; He, X.; Komy, Z. R.; Ismail, N. M.; Dionysiou, D. D. Revealing 674 the Mechanism, Pathways and Kinetics of UV 254nm/H₂O₂-Based Degradation of Model 675 Active Sunscreen Ingredient PBSA. *Chem. Eng. J.* **2016**, *288*, 824–833.
- 676 (56) Kraljić, I.; Sharpatyi, V. A. Determination of Singlet Oxygen Rate Constants in Aqueous Solutions. *Photochem. Photobiol.* **1978**, *28* (4–5), 583–586.
- 678 (57) Ching, T.-L.; Haenen, G. R. M. M.; Bast, A. Cimetidine and Other H₂ Receptor Antagonists as Powerful Hydroxyl Radical Scavengers. *Chem. Biol. Interact.* **1993**, *86* (2), 119–127.

- 680 (58) Mercader, A. G.; Duchowicz, P. R.; Fernández, F. M.; Castro, E. A.; Cabrerizo, F. M.; 681 Thomas, A. H. Predictive Modeling of the Total Deactivation Rate Constant of Singlet 682 Oxygen by Heterocyclic Compounds. *J. Mol. Graph. Model.* **2009**, *28* (1), 12–19.
- 683 (59) Iddon, B.; Phillips, G. O.; Robbins, K. E.; Davies, J. V. Radiation Chemistry of Aqueous Solutions of Indole and Its Derivatives. *J. Chem. Soc. B* **1971**, 6, 1887-1892.
- 685 (60) Kawanishi, S.; Sakurai, H. Differential Anti-Lipid Peroxidative Activity of Melatonin.

 Naturwissenschaften **2002**, 89 (1), 31–33.
- 687 (61) Li, Y. J.; Huang, D. D.; Cheung, H. Y.; Lee, A. K. Y.; Chan, C. K. Aqueous-Phase 688 Photochemical Oxidation and Direct Photolysis of Vanillin – a Model Compound of 689 Methoxy Phenols from Biomass Burning. *Atmospheric Chem. Phys.* **2014**, *14* (6), 2871– 690 2885.
- 691 (62) Machado, A. E. H.; Gomes, A. J.; Campos, C. M. F.; Terrones, M. G. H.; Perez, D. S.; Ruggiero, R.; Castellan, A. Photoreactivity of Lignin Model Compounds in the Photobleaching of Chemical Pulps 2. Study of the Degradation of 4-Hydroxy-3-Methoxy-Benzaldehyde and Two Lignin Fragments Induced by Singlet Oxygen. *J. Photochem. Photobiol. Chem.* 1997, 110 (1), 99–106.

697

698

699

700

701

702

703

704

705

706

709

710

- (63) Tratnyek, P. G.; Hoigne, J. Oxidation of Substituted Phenols in the Environment: A QSAR Analysis of Rate Constants for Reaction with Singlet Oxygen. *Environ. Sci. Technol.* **1991**, *25* (9), 1596–1604.
- (64) Lauraguais, A.; Coeur-Tourneur, C.; Cassez, A.; Seydi, A. Rate Constant and Secondary Organic Aerosol Yields for the Gas-Phase Reaction of Hydroxyl Radicals with Syringol (2,6-Dimethoxyphenol). *Atmos. Environ.* **2012**, *55*, 43–48.
- (65) Scully, F. E.; Hoigné, J. Rate Constants for Reactions of Singlet Oxygen with Phenols and Other Compounds in Water. *Chemosphere* **1987**, *16* (4), 681–694.
- (66) Biswal, J.; Paul, J.; Naik, D. B.; Sarkar, S. K.; Sabharwal, S. Radiolytic Degradation of 4-Nitrophenol in Aqueous Solutions: Pulse and Steady State Radiolysis Study. *Radiat. Phys. Chem.* **2013**, *85*, 161–166.
- 707 (67) Lundeen, R. A.; Janssen, E. M.-L.; Chu, C.; Mcneill, K. Environmental Photochemistry of Amino Acids, Peptides and Proteins. *Chim. Int. J. Chem.* **2014**, *68* (11), 812–817.
 - (68) Mártire, D. O.; Braslavsky, S. E.; García, N. A. Sensitized Photo-Oxidation of Dihydroxybenzenes and Chlorinated Derivatives. A Kinetic Study. *J. Photochem. Photobiol. Chem.* **1991**, *61* (1), 113–124.
- 712 (69) Smith, J. D.; Kinney, H.; Anastasio, Cort. Phenolic Carbonyls Undergo Rapid Aqueous 713 Photodegradation to Form Low-Volatility, Light-Absorbing Products. *Atmos. Environ.* 714 **2016**, *126*, 36–44.
- 715 (70) McConville, M. B.; Mezyk, S. P.; Remucal, C. K. Indirect Photodegradation of the 716 Lampricides TFM and Niclosamide. *Environ. Sci. Process. Impacts* **2017**, *19* (8), 1028– 717 1039.
- (71) Mashayekhy Rad, F.; Zurita, J.; Gilles, P.; Rutgeerts, L. A. J.; Nilsson, U.; Ilag, L. L.; Leck,
 C. Measurements of Atmospheric Proteinaceous Aerosol in the Arctic Using a Selective
 UHPLC/ESI-MS/MS Strategy. J. Am. Soc. Mass Spectrom. 2019, 30 (1), 161–173.
- 721 (72) Teich, M.; Pinxteren, D. van; Wang, M.; Kecorius, S.; Wang, Z.; Müller, T.; Močnik, G.; Herrmann, H. Contributions of Nitrated Aromatic Compounds to the Light Absorption of Water-Soluble and Particulate Brown Carbon in Different Atmospheric Environments in Germany and China. *Atmospheric Chem. Phys.* **2017**, *17* (3), 1653–1672.

- 725 (73) Wang, Y.; Hu, M.; Wang, Y.; Zheng, J.; Shang, D.; Yang, Y.; Liu, Y.; Li, X.; Tang, R.; Zhu, W. The Formation of Nitro-Aromatic Compounds under High NO_x and Anthropogenic VOC Conditions in Urban Beijing, China. *Atmospheric Chem. Phys.* **2019**, 19 (11), 7649–7665.
- 729 (74) Li, Y. J.; Huang, D. D.; Cheung, H. Y.; Lee, A. K. Y.; Chan, C. K. Aqueous-Phase 730 Photochemical Oxidation and Direct Photolysis of Vanillin – a Model Compound of 731 Methoxy Phenols from Biomass Burning. *Atmospheric Chem. Phys.* **2014**, *14* (6), 2871– 732 2885.
- 733 (75) Vione, D.; Albinet, A.; Barsotti, F.; Mekic, M.; Jiang, B.; Minero, C.; Brigante, M.; 734 Gligorovski, S. Formation of Substances with Humic-like Fluorescence Properties, upon Photoinduced Oligomerization of Typical Phenolic Compounds Emitted by Biomass Burning. *Atmos. Environ.* **2019**, *206*, 197–207.
- 737 (76) Cory, R. M.; McNeill, K.; Cotner, J. P.; Amado, A.; Purcell, J. M.; Marshall, A. G. Singlet 738 Oxygen in the Coupled Photochemical and Biochemical Oxidation of Dissolved Organic 739 Matter. *Environ. Sci. Technol.* **2010**, *44* (10), 3683–3689.
- (77) Badali, K. M.; Zhou, S.; Aljawhary, D.; Antiñolo, M.; Chen, W. J.; Lok, A.; Mungall, E.;
 Wong, J. P. S.; Zhao, R.; Abbatt, J. P. D. Formation of Hydroxyl Radicals from Photolysis of Secondary Organic Aerosol Material. *Atmos Chem Phys* 2015, *15* (14), 7831–7840.